Available online at www.sciencedirect.com
ScienceDirect
Comput. Methods Appl. Mech. Engrg. 196 (2006) 489–501
Computer methods in applied mechanics and engineering
www.elsevier.com/locate/cma

On the computation of the derivatives of potentials on a boundary by using boundary-integral equations

A. Sellier *

LadHyX, Ecole polytechnique, 91128 Palaiseau Cédex, France

Received 17 May 2005; received in revised form 6 February 2006; accepted 10 May 2006

Abstract

This work presents a new recursion scheme to compute the cartesian derivatives of potentials on the smooth surface of a connected solid. The advocated strategy solely appeals to boundary-integral equations and a very few informations regarding the surface geometry. The whole algorithm is carefully tested against analytical solutions both for interior and exterior problems by implementing a collocation points method.

Keywords: Harmonic function; Boundary-integral equation; Boundary element method

1. Introduction

Let us consider a solid particle occupying the bounded domain $\mathscr{P}$ enclosed by a smooth, insulating and closed surface S, of unit outward normal $\mathbf{n}$, immersed in a viscous and conducting liquid metal. It has been shown [1] that when subject to uniform ambient electric and magnetic fields $\mathbf{E}$ and $\mathbf{B}$ this particle experiences a rigid-body motion whose determination requires to calculate surface integrals of the following types

$$I_1 = \int_S [V_i \phi_{,i}](\mathbf{x})\,\mathrm{d}S(\mathbf{x}), \quad I_2 = \int_S [W_{ij}\phi_{,ij}](\mathbf{x})\,\mathrm{d}S(\mathbf{x}), \tag{1}$$

where ϕ denotes the perturbation electrostatic potential, harmonic in the unbounded fluid domain $\Omega = \mathbb{R}^3 \setminus \mathscr{P}$ and subject to the Neumann boundary condition $\nabla\phi \cdot \mathbf{n} = \mathbf{E} \cdot \mathbf{n}$ on the insulating surface S and $\phi_{,i} = \partial\phi/\partial x_i$ whereas $\phi_{,ij} = \partial^2\phi/\partial x_i \partial x_j$ for usual Cartesian coordinates $x_i = \mathbf{OM} \cdot \mathbf{e}_i$. In addition, occurring vector or tensor cartesian components V_i or W_{ij} in (1) are given. Clearly, the key evaluation of I_1 and I_2 appeals to accurate approximations of $\phi_{,i}$ and $\phi_{,ij}$ on the boundary S. At a very first glance, one may think about estimating I_1 by the determination of ϕ on S (as explained in Section 2.1) and the computation of its tangential derivatives (because we know the normal component $\nabla\phi \cdot \mathbf{n} = \mathbf{E} \cdot \mathbf{n}$ this procedure indeed provides the required potential gradient, $\nabla\phi$, on the surface). However, such an approximation of the needed tangential gradient, $\nabla\phi - [\nabla\phi \cdot \mathbf{n}]\mathbf{n}$, requires to resort to high-order boundary elements on S. For example, using 6-node (curvilinear) triangular boundary elements yields a linear approximation of the tangential gradient but only at interior points of the elements. If one may content oneself with this procedure for I_1 the case of I_2 is far more tricky: if indeed it remains possible to deduce inner constant approximations of second-order tangential derivatives of ϕ on each quadratic boundary element (such as previously alluded to 6-node curvilinear triangular elements) the obtention of the needed second-order normal derivatives, by exploiting $\nabla^2\phi = 0$ on S, necessarily requires the intricated use of local coordinates (as achieved in [2–4]). In the same spirit, the calculation of the third-order derivatives $\phi_{,ijk}$ would at least require to resort to cubic interpolations of ϕ on S and a cumbersome link for the third-order normal derivative in terms of local coordinates. Accordingly, one needs another

* Tel.: +33 1 69 33 36 79; fax: +33 1 69 33 30 30.
E-mail address: sellier@ladhyx.polytechnique.fr

0045-7825/$ - see front matter © 2006 Elsevier B.V. All rights reserved.
doi:10.1016/j.cma.2006.05.003

procedure in computing high-order derivatives of the potential on the surface. One might object that, except for the motivating cases of I_1 and I_2, one seldom needs to compute the derivatives of potentials on the surface. However, it is sometimes worth evaluating ϕ and/or its derivatives not on but near to S and the well-known and widely employed integral representations of $\phi(M)$ and its derivatives, in terms of the values of ϕ and the normal flux $\nabla\phi\cdot\mathbf{n}$ on S (see Section 2), experience dramatic losses of accuracy as M approaches S. Even more and more refined surface meshes fail in adequately handling such difficulties. To remedy to these troubles it seems quite suitable to appeal to the Taylor expansion of ϕ about a point M_0 of S close to M and this approach rests on the accurate estimation of more and more higher order cartesian derivatives of ϕ at this point M_0 on S, at least is $\mathbf{M}_0\mathbf{M}$ is not parallel to $\mathbf{n}(M_0)$. Similar worries actually also arise in linear elasticity for the key evaluation of the surface stresses near or on a boundary. If most of available papers deal with an hyper-singular boundary-integral equation for the required stress Cartesian components [5–8] and the displacement Cartesian derivatives [9] note that [10] and [11] end up with a non-singular boundary-integral equation in 2D and 3D problems, respectively.

Recently [2–4] proposed a general method to compute derivatives of potentials, displacements, stresses on the boundary in both 2D and 3D problems arising in potential theory and linear elasticity. The approach resorts to local curvilinear normal and tangent coordinates in a neighborhood of S and notes that each normal derivative $\partial^k\phi/\partial n^k$ (of order $k\geqslant 2$) may be expressed, by exploiting the harmonic equation, in terms of tangential derivatives of order $k-l$ of the normal derivatives $\partial^l\phi/\partial n^l$ for $0\leqslant l\leqslant k-1$, (under the notation $\partial^0\phi/\partial n=\phi$). Hence, on S the derivatives (with respect to the local coordinates) up to order $k\geqslant 2$ are deduced from tangential derivatives of ϕ and $\psi=\nabla\phi\cdot\mathbf{n}$ up to order k and $k-1$ respectively. It is proved that, writing the integral representation $A[\psi]=B[\phi]$ on S, each tangential derivative of ψ of order $m\geqslant 1$, denoted by $\psi_t^{(m)}$, fulfills the boundary-integral equation $A[\psi_t^{(m)}]=C_m$ on S, with C_m obtained from $\phi_t^{(m)},\psi$ and $\psi_t^{(l)}$ with $2\leqslant l\leqslant m-2$ if $m\geqslant 2$. Successively solving such integral equations as m increases from 1 to $k-1$ ($k\geqslant 2$) thus provides on S the derivatives of ϕ *with respect to local coordinates* up to order k. To the present day, this procedure has been successfully and numerically worked out for $k=2$ (by a Galerkin method) and 2D interior or exterior Dirichlet problems for the Laplace and plane linear elasticity equations only. Actually, the numerical implementation for $k\geqslant 3$ and/or 3D problems encounters the following difficulties:

(i) For $k\geqslant 3$, one needs accurate approximations of higher and higher order tangential derivatives of both ϕ and the local metric tensor on S. Even if the surface is analytically given this requires more and more calculations and when ϕ is not analytically prescribed more and more refined meshes on S since one then also needs to numerically approximate ϕ on the boundary.
(ii) One has to build the encountered right-hand sides C_m, a task which becomes involved as m increases.
(iii) In 3D cases two tangential coordinates are needed and this results in a tedious calculation of C_m, even for $k=2$.
(iv) Finally, the obtained derivatives are expressed in local coordinates only. This appears somewhat damaging for subsequent use of these derivatives (for instance for surface integrations of derivatives, as needed for I_1 and I_2) or Taylor's expansions of both the potential and its derivatives in the vicinity of the boundary.

This work presents a new procedure free from all the previous drawbacks (ii)–(iv). The advocated treatment gives the *cartesian* derivatives $\phi_{,i_1\ldots i_m}$, if needed up to large orders $m\geqslant 1$, without any amount of complexity as m increases and solely makes use of the unit normal vector $\mathbf{n}$ and the mean curvature on the surface S. More precisely, the paper is organized as follows. A new boundary-integral equation and a suitable bootstrapping algorithm that provides the cartesian derivatives of ϕ up to order $m\geqslant 1$ are established in Section 2, both for interior and exterior problems and a the surface S of one connected solid. The general case of the surface of a collection of connected solids is addressed in Section 3 whereas a numerical implementation and illustrating benchmarks, both for one and several connected solids, are presented in Section 4. Finally, a few concluding remarks and suggestions close the paper in Section 5.

2. Interior or exterior problems for one connected body

Let us call connected solid a nonempty, compact and connected subset of $\mathbb{R}^3$ whose smooth boundary S has only one connected component and denote by Ω_i its interior. We further designate by Ω_e the exterior domain $\Omega_e=\mathbb{R}^3\setminus\Omega_i$ and by $\mathbf{n}$ the unit outward normal on S, as sketched in Fig. 1(a) and (b).

Throughout the paper Cartesian coordinates $x_i=\mathbf{OM}\cdot\mathbf{e}_i$ and the usual tensor summation notation are adopted with $\mathbf{x}=\mathbf{OM}=x_i\mathbf{e}_i$ and $r=|\mathbf{x}|=(x_ix_i)^{1/2}$. Both for interior ($\Omega=\Omega_i$) and exterior ($\Omega=\Omega_e$) cases, the poten-

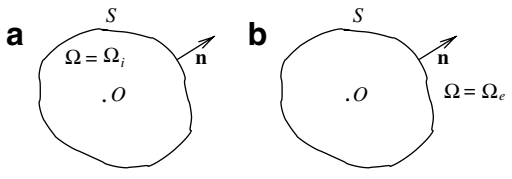

Fig. 1. (a) Case of the interior problem: $\Omega=\Omega_i$. (b) Case of the exterior problem: $\Omega=\Omega_e$.

tial ϕ is governed by the usual mixed boundary value problem

$$\nabla^2\phi = 0 \text{ in } \Omega, \quad \nabla\phi\cdot\mathbf{n} = F \text{ on } S', \quad \phi = U \text{ on } S'' = S\setminus S' \tag{2}$$

with prescribed Neumann and Dirichlet data F and U and the following additional far-field behavior and compatibility condition

$$|r\phi| \leqslant \mathrm{O}(1) \quad \text{as } r\to\infty \text{ for exterior Cases } (\Omega=\Omega_e), \tag{3}$$

$$\int_S F(\mathbf{y})\,\mathrm{d}S(\mathbf{y}) = 0 \quad \text{if } S' = S \text{ for interior Cases } (\Omega=\Omega_i). \tag{4}$$

Let us introduce the usual Sobolev spaces $H^1(\Omega_i) = \{u$ such that $u\in L^2(\Omega_i)$ with $\partial u/\partial x_i \in L^2(\Omega_e)$ for $i=1,2,3\}$, $W(\Omega_e) = \{u$ such that $u/(1+r^2)^{1/2}\in L^2(\Omega_e)$ and $\partial u/\partial x_i \in L^2(\Omega_e)$ for $i=1,2,3\}$, the standard boundary Sobolev space $H^{1/2}(S)$ as alluded-to in [4] and detailed in [15], and its dual Sobolev space $H^{-1/2}(S)$ via the usual L^2-duality. For $\Sigma\subset S$ we furthermore define the dual Sobolev boundary spaces $H^{1/2}(\Sigma)$ and $H^{-1/2}(\Sigma)$ with $H^{1/2}(\Sigma) = \{u$ defined on Σ such that $\hat{u}\in H^{1/2}(S)$ if $\hat{u} = u$ on Σ and $\hat{u} = 0$ on $S\setminus\Sigma\}$. Then [12], under the additional conditions (3) or (4), the problem (2) admits a unique solution ϕ in $W(\Omega_e)$ or $H^1(\Omega_i)$ as soon as $U\in H^{1/2}(S'')$ and $F\in H^{-1/2}(S')$ for exterior problems or interior problems respectively if $S\neq S'$. If $S' = S$ any well-posed interior problem (such that the compatibility condition (4) holds) admits a solution $\phi\in H^1(\Omega)$ unique up to an arbitrary constant for $F\in H^{-1/2}(S)$. For any encountered case, we look at the cartesian derivatives $\phi_{,i} = \partial\phi/\partial x_i$, $\phi_{,ij} = (\phi_{,i})_{,j}$, ...at the boundary S.

2.1. Obtention of the normal flux on the surface

In this subsection it is assumed that $S'\neq S$ and we briefly give a well-established procedure to obtain the potential ϕ and its normal flux $\nabla\phi\cdot\mathbf{n}$ on the whole boundary. If $G(\mathbf{x},\mathbf{y})$, $H(\mathbf{x},\mathbf{y}) = \nabla G_{\mathbf{y}}\cdot\mathbf{n}(\mathbf{y})$ and $h(\mathbf{x})$ respectively denote the usual free space Green's function, its normal derivative on the surface S and a function h such that

$$G(\mathbf{x},\mathbf{y}) = \frac{1}{4\pi|\mathbf{x}-\mathbf{y}|}, \quad H(\mathbf{x},\mathbf{y}) = \frac{(\mathbf{x}-\mathbf{y})\cdot\mathbf{n}(\mathbf{y})}{4\pi|\mathbf{x}-\mathbf{y}|^3},$$
$$h(\mathbf{x}) = \int_S H(\mathbf{x},\mathbf{y})\,\mathrm{d}S(\mathbf{y}) \tag{5}$$

we first note that, because S admits a tangent plane everywhere,

$$h(\mathbf{x}) = -1 \text{ if } \mathbf{x}\in\Omega_i, \quad h(\mathbf{x}) = -1/2 \text{ if } \mathbf{x}\in S,$$
$$h(\mathbf{x}) = 0 \text{ if } \mathbf{x}\in\Omega_e. \tag{6}$$

In addition, the second Green's identity yields the widely employed integral representation

$$\int_S \{G(\mathbf{x},\mathbf{y})[\nabla\phi\cdot\mathbf{n}](\mathbf{y}) - \phi(\mathbf{y})H(\mathbf{x},\mathbf{y})\}\,\mathrm{d}S(\mathbf{y}) = \mp\phi(\mathbf{x}), \quad \text{for } \mathbf{x}\in\Omega \tag{7}$$

with, as henceforth adopted in the whole paper, signs $-$ or $+$ for interior or exterior problems respectively. If Ω is bounded (case of the interior problem) the above property (7) easily arises (see [13,14]) from the basic link $\nabla^2 G(\mathbf{x},\mathbf{y}) + \delta(\mathbf{y}-\mathbf{x}) = 0$ where δ denotes the usual Dirac generalized function. For exterior problems one introduces, as depicted in Fig. 2, the bounded domain Ω_ρ enclosed by S and the sphere $S_\rho = \{\mathbf{y}; |\mathbf{y}-\mathbf{x}| = \rho\}$ centered at $\mathbf{x}\in\Omega = \Omega_e$ and of large enough radius ρ. Relation (7) then holds for the interior problem in Ω_ρ of boundary $S\cup S_\rho$ and outwarding unit normal $\mathbf{e}_{\mathbf{x}}(\mathbf{y}) = (\mathbf{y}-\mathbf{x})/\rho$ on S_ρ and $-\mathbf{n}$ on S. Noting that the far-field behavior (3) and the $1/r$-decay of G make the integration on S_ρ vanish as ρ tends to infinity, one thus deduces (7) for the exterior problem.

For interior problems, substituting (6) in (7) then yields

$$\int_S \{G(\mathbf{x},\mathbf{y})[\nabla\phi\cdot\mathbf{n}](\mathbf{y}) - [\phi(\mathbf{y})-\phi(\mathbf{x})]H(\mathbf{x},\mathbf{y})\}\,\mathrm{d}S(\mathbf{y}) = 0, \quad \text{for } \mathbf{x}\in\Omega_i\cup S. \tag{8}$$

Indeed, (8) clearly holds if $\mathbf{x}$ belongs to $\Omega = \Omega_i$ and it actually remains true as $\mathbf{x}$ tends to S because each occurring integral remains regular in such a limit process. The case of exterior problems is again handled by using the bounded domain Ω_ρ and letting ρ tend to infinity. Noting that for $\mathbf{x}\in\Omega_\rho\cup S$

$$\int_{S_\rho} \frac{(\mathbf{x}-\mathbf{y})\cdot\mathbf{e}_{\mathbf{x}}(\mathbf{y})}{|\mathbf{x}-\mathbf{y}|^3}\,\mathrm{d}S(\mathbf{y}) = -4\pi, \tag{9}$$

one this time ends up, for any exterior problem, with the relation

$$\int_S \{G(\mathbf{x},\mathbf{y})[\nabla\phi\cdot\mathbf{n}](\mathbf{y}) - [\phi(\mathbf{y})-\phi(\mathbf{x})]H(\mathbf{x},\mathbf{y})\}\,\mathrm{d}S(\mathbf{y}) = -\phi(\mathbf{x}), \quad \text{for } \mathbf{x}\in\Omega_e\cup S. \tag{10}$$

If $\mathbf{x}$ is located on S the above links (8) and (10) result in boundary-integral equations that relate the potential ϕ to its normal flux $\nabla\phi\cdot\mathbf{n}$ on the boundary. More precisely, taking into account the mixed boundary value conditions

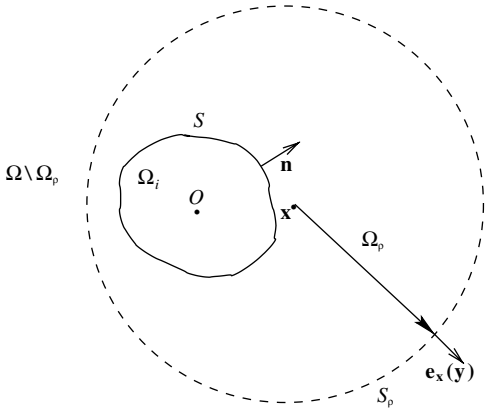

Fig. 2. Case of an exterior problem. The surface, S_ρ, of the sphere centered at $\mathbf{x}$ is indicated by the dashed curve.

(2) on $S' \neq S$ and S'', one obtains the well-posed boundary-integral equation

$$\int_S [\phi(\mathbf{y}) - \phi(\mathbf{x})] \frac{(\mathbf{x}-\mathbf{y})\cdot\mathbf{n}(\mathbf{y})}{|\mathbf{x}-\mathbf{y}|^3}\,dS(\mathbf{y}) - 2\pi(1^+_-1)\phi(\mathbf{x}) = \int_S \frac{[\nabla\phi\cdot\mathbf{n}](\mathbf{y})}{|\mathbf{x}-\mathbf{y}|}\,dS(\mathbf{y}), \quad \mathbf{x}\in S \tag{11}$$

with $-$ and $+$ signs for interior and exterior problems respectively. Each integral occurring in (11) is regular and the boundary-integral equation (11) admits a unique solution $\phi \in H^{1/2}(S)$, $\nabla\phi\cdot\mathbf{n} \in H^{-1/2}(S)$ as soon as $S' \neq S$ if $\nabla\phi\cdot\mathbf{n} = F \in H^{-1/2}(S')$ and $\phi = U \in H^{1/2}(S'')$. If one resorts to a N-node mesh on S (for example for a collocation point implementation as achieved in Section 4) and denotes by $g(n)$ the value of the function g at the nth node $M(n)$, the discretized Eq. (11) provides N relations for the generalized $2N$-unknown $X = (\phi(1),\ldots,\phi(N);\ [\nabla\phi\cdot\mathbf{n}](1),\ldots,[\nabla\phi\cdot\mathbf{n}](N))$ whereas the boundary conditions (3) provide N additional relations: $\phi(M(n)) = U$ and $[\nabla\phi\cdot\mathbf{n}](M(n)) = F$ if $M(n)$ belongs to S'' and S' respectively. In summary, we now assume that ϕ and its normal flux $F = \nabla\cdot\mathbf{n}$ are given on the whole surface S, i.e. on a prescribed N-node mesh of S.

2.2. Obtention of the potential gradient on the surface

This subsection establishes the key boundary-integral equation that permits us to deduce the cartesian components $\phi_{,i} = \nabla\phi\cdot\mathbf{e}_i$ of the gradient on S from the previous knowledge of the normal flux $F = \nabla\phi\cdot\mathbf{n}$ and a very few informations on the geometry. We successively present and prove the boundary-integral equation of interest.

The surface is smooth enough so that it admits continuous normal $\mathbf{n}(\mathbf{x}) = n_i(\mathbf{x})\mathbf{e}_i$ and mean curvature $H_c(\mathbf{x}) := -C(\mathbf{x})/2$ with $C(\mathbf{x}) = [\nabla\cdot\mathbf{n}](\mathbf{x})$ (for these latter definitions of differential operators on the surface S the reader is directed to [15]). For $\mathbf{x}$ on S such assumptions make it possible to introduce, for $i\in\{1,2,3\}$, the surface integrals

$$I_i(\mathbf{x},S) = \int_S \left[\frac{(\mathbf{y}-\mathbf{x})\cdot\mathbf{n}(\mathbf{y})}{|\mathbf{x}-\mathbf{y}|^2} - C(\mathbf{y})\right]\frac{\mathbf{n}(\mathbf{y})\cdot\mathbf{e}_i}{|\mathbf{x}-\mathbf{y}|}\,dS(\mathbf{y}),$$
$$C(\mathbf{x}) = [\nabla\cdot\mathbf{n}](\mathbf{x}). \tag{12}$$

Each above integral $I_i(\mathbf{x},S)$, that only depends upon $\mathbf{x}$ and the geometry, indeed is regular since (6) yields for $\mathbf{x}$ on S

$$\int_S \left[\frac{(\mathbf{y}-\mathbf{x})\cdot\mathbf{n}(\mathbf{y})}{2\pi|\mathbf{x}-\mathbf{y}|^2}\right]\frac{\mathbf{n}(\mathbf{y})\cdot\mathbf{e}_i\,dS(\mathbf{y})}{|\mathbf{x}-\mathbf{y}|} = n_i(\mathbf{x}) + \int_S \left[\frac{(\mathbf{y}-\mathbf{x})\cdot\mathbf{n}(\mathbf{y})}{2\pi|\mathbf{x}-\mathbf{y}|^3}\right][n_i(\mathbf{y}) - n_i(\mathbf{x})]\,dS(\mathbf{y}). \tag{13}$$

For any function g differentiable in a neighborhood of S let us also define, as in [16], the tangential derivative $D_{ij}g$ on S as

$$[D_{ij}g](\mathbf{y}) = n_i(\mathbf{y})g_{,j}(\mathbf{y}) - n_j(\mathbf{y})g_{,i}(\mathbf{y}) = (\mathbf{e}_i\wedge\mathbf{e}_j)\cdot(\mathbf{n}\wedge\nabla g)[\mathbf{y}]. \tag{14}$$

The last equality (14) indeed clearly shows that $[D_{ij}g](\mathbf{x})$ solely involves tangential derivatives of g at the point $\mathbf{x}$ of S.

Theorem. *If the surface S and the potential ϕ satisfy the assumptions*

(i) *The boundary S admits continuous normal $\mathbf{n}$ and mean curvature C.*

(ii) *The potential is of $C^{1,\alpha+1}$ regularity at any point $\mathbf{x}$ of S, i.e. there exist $\alpha>0$, $C_1>0$ and $C_2>0$ such that for $\mathbf{y}$ on S and close enough to $\mathbf{x}$*

$$|\phi(\mathbf{y}) - \phi(\mathbf{x}) - \nabla\phi(\mathbf{x})\cdot(\mathbf{y}-\mathbf{x})| < C_1|\mathbf{x}-\mathbf{y}|^{1+\alpha},$$
$$|\nabla\phi(\mathbf{y}) - \nabla\phi(\mathbf{x})| < C_2|\mathbf{x}-\mathbf{y}|^{\alpha}, \tag{15}$$

then the following boundary-integral equations govern, for $i\in\{1,2,3\}$, the required potential gradient $\nabla\phi = \phi_{,i}\mathbf{e}_i$

$$\pm 2\pi\phi_{,i}(\mathbf{x}) - [D_{ij}\phi](\mathbf{x})I_j(\mathbf{x},S) + \int_S \left\{\frac{[D_{ij}\phi](\mathbf{y}) - [D_{ij}\phi](\mathbf{x})}{|\mathbf{x}-\mathbf{y}|^3}\right\}(\mathbf{x}-\mathbf{y})\cdot\mathbf{e}_j\,dS(\mathbf{y}) = -F(\mathbf{x})I_i(\mathbf{x},S) + \int_S \left[\frac{F(\mathbf{y})-F(\mathbf{x})}{|\mathbf{x}-\mathbf{y}|^3}\right](\mathbf{x}-\mathbf{y})\cdot\mathbf{e}_i\,dS(\mathbf{y}), \quad \mathbf{x}\in S \tag{16}$$

with signs $-$ or $+$ for interior or exterior problems respectively and a normal flux $F(\mathbf{x}) = [\nabla\phi\cdot\mathbf{n}](\mathbf{x})$ given on the whole surface S (as explained in Section 2.1).

Proof. The derivation of (16) is achieved in three steps and, for conciseness, omitted details and elementary calculations are displayed in Appendix A.

Step 1: Since it concentrates all the difficulties we first consider an exterior problem and introduce for $\mathbf{x}\in\Omega\cup S$ the potentials $\psi(\mathbf{y}) = \phi(\mathbf{x}) + \nabla\phi(\mathbf{x})\cdot(\mathbf{y}-\mathbf{x})$ and $\psi_j(\mathbf{y}) = (\mathbf{y}-\mathbf{x})\cdot\mathbf{e}_j$. Of course, $\psi(\mathbf{y})$ and $\psi_j(\mathbf{y})$ are harmonic in Ω but do not exhibit the 'good' far-field behavior (3), previously invoked in establishing (10). Again we resort to the bounded domain Ω_ρ (see Fig. 2) and apply (8) to ψ and ψ_j for this domain. We then end up with two surface integrals: one over S and the other one over S_ρ. Keeping the notations $\rho = |\mathbf{y}-\mathbf{x}|$ and $\mathbf{e}_\mathbf{x}(\mathbf{y}) = (\mathbf{y}-\mathbf{x})/\rho$ and invoking symmetries we easily obtain

$$\int_{S_\rho} [\nabla\psi\cdot\mathbf{n}](\mathbf{y})G(\mathbf{x},\mathbf{y})\,dS(\mathbf{y}) = \int_{S_\rho} \frac{\nabla\phi(\mathbf{x})\cdot\mathbf{e}_\mathbf{x}(\mathbf{y})\,dS(\mathbf{y})}{4\pi\rho} = 0, \tag{17}$$

$$\int_{S_\rho} [\nabla\psi_j\cdot\mathbf{n}](\mathbf{y})G(\mathbf{x},\mathbf{y})\,dS(\mathbf{y}) = \int_{S_\rho} \frac{\mathbf{e}_j\cdot\mathbf{e}_\mathbf{x}(\mathbf{y})\,dS(\mathbf{y})}{4\pi\rho} = 0, \tag{18}$$

$$\int_{S_\rho} [f(\mathbf{y}) - f(\mathbf{x})]H(\mathbf{x},\mathbf{y})\,dS(\mathbf{y}) = 0 \quad \text{for } f=\psi \text{ and } f=\psi_j. \tag{19}$$

Accordingly, the integral on S_ρ vanishes and the relation (8) also holds for ψ and ψ_j! More precisely, from the definition of ψ_j it follows that

$$\int_S \{n_j(\mathbf{y})G(\mathbf{x},\mathbf{y}) - (\mathbf{y}-\mathbf{x})\cdot\mathbf{e}_j H(\mathbf{x},\mathbf{y})\}\,\mathrm{d}S(\mathbf{y}) = 0 \quad \text{for } \mathbf{x}\in\Omega\cup S, \tag{20}$$

whereas the combination of (10) for ϕ with (8) for ψ immediately provides, under the definition of ψ, the regularized relation

$$\phi(\mathbf{x}) = \int_S \{\phi(\mathbf{y}) - \phi(\mathbf{x}) - \nabla\phi(\mathbf{x}).(\mathbf{y}-\mathbf{x})]\}H(\mathbf{x},\mathbf{y})\,\mathrm{d}S(\mathbf{y}) - \int_S [\nabla\phi(\mathbf{y}) - \nabla\phi(\mathbf{x})]\cdot\mathbf{n}(\mathbf{y})G(\mathbf{x},\mathbf{y})\,\mathrm{d}S(\mathbf{y}) \quad \text{for } \mathbf{x}\in\Omega\cup S. \tag{21}$$

For $\mathbf{x} = x_i\mathbf{e}_i$ and $\mathbf{y} = y_i\mathbf{e}_i$ we set $G_{,i} = \partial H/\partial y_i$ and observe that $G_{,i} = -\partial G/\partial x_i$. From the definition $H = G_{,j}n_j$ one thus obtains $\partial G/\partial x_i = -G_{,ij}n_j$. Exploiting these properties and (20), the derivation of (21) with respect to x_i yields the key identities

$$\phi_{,i}(\mathbf{x}) = \int_S \big\{(\nabla\phi\cdot\mathbf{n})(\mathbf{y}) - (\nabla\phi\cdot\mathbf{n})(\mathbf{x}) - \nabla\phi(\mathbf{x})\cdot[\mathbf{n}(\mathbf{y})-\mathbf{n}(\mathbf{x})]\big\}G_{,i}(\mathbf{x},\mathbf{y})\,\mathrm{d}S(\mathbf{y}) + \int_S [\phi(\mathbf{x}) - \phi(\mathbf{y}) - \nabla\phi(\mathbf{x})\cdot(\mathbf{x}-\mathbf{y})] \times G_{,ij}(\mathbf{x},\mathbf{y})n_j(\mathbf{y})\,\mathrm{d}S(\mathbf{y}) \quad \text{for } \mathbf{x}\in\Omega\cup S. \tag{22}$$

Let us emphasize that (21) and (22) not only hold in Ω but also on the boundary. As the reader may easily check, under assumptions (i) and (ii) each integral in (22) is regular for $\mathbf{x}$ on S. Note that (22) turns out to be a boundary-integral equation for $\nabla\phi$ on S as soon as one knows ϕ and its normal flux $\nabla\phi\cdot\mathbf{n}$ on the boundary. As achieved in steps 2 and 3 it is however possible to restrict the needed surface quantities to $\mathbf{n}$, $\nabla\phi\cdot\mathbf{n}$ and the mean curvature C.

Step 2: For $0<\epsilon\ll 1$ let us introduce, for $\mathbf{x}$ on S, the open set $d_\epsilon = \{\mathbf{y}\in S,\ |\mathbf{x}-\mathbf{y}|<\epsilon\}$ and denote by T_1^ϵ and T_2^ϵ the first and second integrals on the right-hand side of (22) with the domain S replaced by $S(\epsilon) = S\backslash d_\epsilon$. Of course, (22) now reads: $\phi_{,i}(\mathbf{x}) = \lim_{\epsilon\to 0}(T_1^\epsilon + T_2^\epsilon)$. Setting

$$K_{ij}^\epsilon(\mathbf{x}) = \int_{S(\epsilon)} n_i(\mathbf{y})G_{,j}(\mathbf{x},\mathbf{y})\,\mathrm{d}S(\mathbf{y}),$$
$$J_i^\epsilon(\mathbf{x}) = \int_{S(\epsilon)} G_{,i}(\mathbf{x},\mathbf{y})\,\mathrm{d}S(\mathbf{y}), \tag{23}$$

one immediately obtains, for $F(\mathbf{x}) = [\nabla\phi\cdot\mathbf{n}](\mathbf{x})$, the decomposition

$$T_1^\epsilon = \int_{S(\epsilon)} [F(\mathbf{y}) - F(\mathbf{x})]G_{,i}(\mathbf{x},\mathbf{y})\,\mathrm{d}S(\mathbf{y}) + F(\mathbf{x})J_i^\epsilon(\mathbf{x}) - \phi_{,j}(\mathbf{x})K_{ji}^\epsilon(\mathbf{x}). \tag{24}$$

From our definition (14) a few elementary algebra yields

$$G_{,ij}(\mathbf{x},\mathbf{y})n_j(\mathbf{y}) = G_{,jj}(\mathbf{x},\mathbf{y})n_i(\mathbf{y}) - D_{ij}[G_{,j}],$$
$$D_{ij}[fg] = fD_{ij}[g] + gD_{ij}[f]. \tag{25}$$

Since $G_{,jj}(\mathbf{x},\mathbf{y}) = 0$ for $\mathbf{y}$ on $S(\epsilon)$ one thus deduces the decomposition

$$T_2^\epsilon = \int_{S(\epsilon)} \big\{G_{,j}D_{ij}[f] - D_{ij}[G_{,j}f]\big\}\,\mathrm{d}S(\mathbf{y}),$$
$$f = \phi(\mathbf{x}) - \phi(\mathbf{y}) - \nabla\phi\cdot(\mathbf{x}-\mathbf{y}). \tag{26}$$

Exploiting the above definition of f, one further obtains

$$D_{ij}[f] = [D_{ij}\phi](\mathbf{x}) - [D_{ij}\phi](\mathbf{y}) + \phi_{,j}(\mathbf{x})n_i(\mathbf{y}) - \phi_{,i}(\mathbf{x})n_j(\mathbf{y}) - [D_{ij}\phi](\mathbf{x}). \tag{27}$$

Appealing to (6) for $\mathbf{x}$ on S and the definition (23) of $K_{ij}^\epsilon(\mathbf{x})$ one thus arrives at

$$T_2^\epsilon = \int_{S(\epsilon)} \big\{[D_{ij}\phi](\mathbf{x}) - [D_{ij}\phi](\mathbf{y})\big\}G_{,j}(\mathbf{x},\mathbf{y})\,\mathrm{d}S(\mathbf{y}) + \phi_{,i}(\mathbf{x})/2 + \phi_{,j}(\mathbf{x})K_{ij}^\epsilon(\mathbf{x}) - [D_{ij}\phi](\mathbf{x})J_j^\epsilon(\mathbf{x}) - \int_{S(\epsilon)} D_{ij}[fG_{,j}]\,\mathrm{d}S(\mathbf{y}) + \phi_{,i}(\mathbf{x})\int_{d(\epsilon)} G_{,j}(\mathbf{x},\mathbf{y})n_j(\mathbf{y})\,\mathrm{d}S(\mathbf{y}). \tag{28}$$

Step 3: We equip the closed boundary c_ϵ of d_ϵ (which is not a circle centered at $\mathbf{x}$) with its unit outward normal $\mathbf{v}$ and tangential vector $\mathbf{t} = \mathbf{n}\wedge\mathbf{v}$. As shown in Appendix A, the Stokes theorem ensures that

$$4\pi\lim_{\epsilon\to 0}[J_i^\epsilon(\mathbf{x})] = -I_i(\mathbf{x},S) + \lim_{\epsilon\to 0}\left[\oint_{c_\epsilon}\frac{\mathbf{e}_i\cdot\mathbf{v}\,\mathrm{d}s(\mathbf{y})}{\rho}\right] \tag{29}$$

where $\rho = |\mathbf{x}-\mathbf{y}|$ and $\mathrm{d}s$ is the differential arc length on the closed path c_ϵ. The first integral on the right-hand side of (24) or (28) are regular as ϵ vanishes. Accordingly, if we rewrite the stated relation (16) as $L_i(\mathbf{x}) = 2\pi\phi_{,i}(\mathbf{x}) + D[\nabla\phi] - E[F] = 0$ we finally deduce from (24) and (28) that

$$L_i(\mathbf{x}) = \lim_{\epsilon\to 0}\{[A_i^{0,\epsilon} + \phi_{,i}A_i^{1,\epsilon} + \phi_{,j}P_{ij}^\epsilon](\mathbf{x})\},$$
$$A_i^{0,\epsilon}(\mathbf{x}) = -4\pi\int_{S(\epsilon)} D_{ij}[fG_{,j}]\,\mathrm{d}S(\mathbf{y}), \tag{30}$$

$$A_i^{1,\epsilon}(\mathbf{x}) = \int_{d(\epsilon)} 4\pi G_{,j}(\mathbf{x},\mathbf{y})n_j(\mathbf{y})\,\mathrm{d}S(\mathbf{y}) + \oint_{c_\epsilon}\frac{n_j(\mathbf{x})\mathbf{e}_j\cdot\mathbf{v}\,\mathrm{d}s(\mathbf{y})}{\rho}, \tag{31}$$

$$P_{ij}^\epsilon(\mathbf{x}) = \int_{S(\epsilon)} 4\pi[n_i(\mathbf{y})G_{,j} - n_j(\mathbf{y})G_{,i}]\,\mathrm{d}S(\mathbf{y}) + \oint_{c_\epsilon}[n_j(\mathbf{x})\mathbf{e}_i\cdot\mathbf{v} - n_i(\mathbf{x})\mathbf{e}_j\cdot\mathbf{v}]\frac{\mathrm{d}s(\mathbf{y})}{\rho}. \tag{32}$$

Because (see Appendix A for details) all quantities $A_i^{0,\epsilon}(\mathbf{x}), A_i^{1,\epsilon}(\mathbf{x})$ and $P_{ij}^\epsilon(\mathbf{x})$ vanish as ϵ goes to zero, we end up with (16) for the exterior problem. For interior potentials note that ψ and ψ_j of course fulfill (8) whereas (21) and (22) hold with left-hand sides $\phi(\mathbf{x})$ and $\phi_{,i}(\mathbf{x})$ replaced with zero. Hence, (16) is also proved for interior problems.

The key relation (16) may be understood as an integral representation of the gradient at the surface: namely, from the knowledge of ϕ and the normal flux $F = \nabla\phi\cdot\mathbf{n}$ one should deduce the value of $\nabla\phi$ on S. Unfortunately, within this point of view one faces with troubles in a numerical

implementation due to the need of adequate and *consistent* interpolations of ϕ and F on the boundary elements. More precisely, in establishing (16) we actually assumed that ϕ and F are $C^{1,\alpha}$ and $C^{0,\alpha}$ on S and if it is easy to obtain $C^{0,\alpha}$ approximations of F, i.e. such that $|F(\mathbf{y})-F(\mathbf{x})|<C_3|\mathbf{y}-\mathbf{x}|^{\alpha}$ for $\mathbf{x}$, $\mathbf{y}$ on S and $C_3>0$, $\alpha>0$, it is tedious to build $C^{1,\alpha}$ approximations of ϕ on boundary elements for a 3D problems. In order to circumvent such damaging drawbacks in any numerical implementation, we rather exploit (16) as a Fredholm boundary-integral equation of the second kind for the gradient $\nabla\phi$ once $\mathbf{n}$, C and the normal flux F are given on S. In this approach we only need $C^{0,\alpha}$ approximations of F; a criterion fulfilled by any usual boundary elements. □

2.3. A boostrapping algorithm for high-order cartesian derivatives

In this subsection we show how to obtain on the N-node mesh of S high-order cartesian derivatives of the potential by a recursion scheme. More precisely, for $m\geqslant 2$ we assume that:

> *Assumption* 1: $\mathbf{n}$ and C are known on the N-node mesh,
> *Assumption* 2: all cartesian derivatives $\phi_{,i_1\ldots i_{m-1}}$ of order $m-1$ are known on the N-node mesh (as explained in Section 2.2 for $m=2$), and we look at the cartesian derivatives $\phi_{,i_1\ldots i_m}$ of order m on the *same* N-node mesh.

For any given values of indices $i_1,\ldots,i_{m-1}$ in the set $\{1,2,3\}$ the required derivatives $\phi_{,i_1\ldots i_{m-1}i_m}$ is obtained, for $i_m\in\{1,2,3\}$, by appealing to the following steps:

Step 1: Obtention of the normal flux $\nabla\phi_{,i_1\ldots i_{m-1}}\cdot\mathbf{n}$ on the N-node mesh.

First we note that our function $\phi_{,i_1\ldots i_{m-1}}$ actually fulfills the well-posed boundary value problem

$$\nabla^2[\phi_{,i_1\ldots i_{m-1}}]=0 \quad \text{in } \Omega, \quad \phi_{,i_1\ldots i_{m-1}}=U_{i_1\ldots i_{m-1}} \quad \text{on } S, \tag{33}$$

$$|r\phi_{,i_1\ldots i_{m-1}}|\leqslant \mathrm{O}(1) \quad \text{as } r\to\infty \text{ for exterior problems}, \tag{34}$$

with, under our Assumption 2, a prescribed Dirichlet data $U_{i_1\ldots i_{m-1}}$ on S. As explained in Section 2.1, we thus obtain the normal flux $\nabla\phi_{,i_1\ldots i_{m-1}}\cdot\mathbf{n}$ on the given N-node mesh by exploiting (11) which becomes the following Fredholm boundary-integral equation of the first kind

$$B[\nabla\phi_{,i_1\ldots i_{m-1}}\cdot\mathbf{n}]=A_{\pm}[\phi_{,i_1\ldots i_{m-1}}] \quad \text{on } S, \tag{35}$$

with operators A_-, A_+ and B defined as

$$A_{\pm}[u]=-2\pi(1\pm 1)u(\mathbf{x})+\int_S\frac{[u(\mathbf{y})-u(\mathbf{x})](\mathbf{x}-\mathbf{y})\cdot\mathbf{n}\,\mathrm{d}S(\mathbf{y})}{|\mathbf{x}-\mathbf{y}|^3},$$

$$B[u]=\int_S\frac{u(\mathbf{y})\,\mathrm{d}S(\mathbf{y})}{|\mathbf{x}-\mathbf{y}|}. \tag{36}$$

Step 2: Obtention of $\phi_{,i_1\ldots i_{m-1}i_m}$ on the N-node mesh.

Since $\phi_{,i_1\ldots i_{m-1}}$ is harmonic in Ω we deduce its gradient $\nabla\phi_{,i_1\ldots i_{m-1}}=\phi_{,i_1\ldots i_{m-1}i_m}\mathbf{e}_{i_m}$ on the N-node mesh from the value of $\mathbf{n}$, C and the previous normal flux $\nabla\phi_{,i_1\ldots i_{m-1}}\cdot\mathbf{n}$ on S, as explained in Section 2.2. More precisely, we end up with the Fredholm boundary-integral equation of the second kind

$$C_{\pm}[\nabla\phi_{,i_1\ldots i_{m-1}}]=D[\nabla\phi_{,i_1\ldots i_{m-1}}\cdot\mathbf{n}] \quad \text{on } S, \tag{37}$$

where operators $C_{\pm}$ and D are readily defined by inspecting (16). Solving the above Eq. (37) then provides the required cartesian derivatives $\phi_{,i_1\ldots i_{m-1}i_m}$ for prescribed indices $i_1,\ldots,i_{m-1}$ and $i_m\in\{1,2,3\}$ on the N-node mesh.

In summary, the computation up to any order $m\geqslant 2$ and on a given N-node mesh of the cartesian derivatives of ϕ subject to (2)–(4) is achieved by using the following strategy:

(1) Preliminary computational work
  (i) The values of $\mathbf{n}$ and C are prescribed at each nodal point $M(n)$ from an analytical description of the surface (as anyone knows, it is indeed very difficult to accurately compute the required mean curvature C solely from the location of the employed nodes).
  (ii) The integrals $I_i(\mathbf{x},\Omega)$, previously defined by (12), are computed at each node $M(n)$.
  (iii) The discretized integral Eqs. (35) and (37) yields discretized and fully populated $N\times N$ square matrices B and $A_{\pm}$ and $3N\times 3N$ square matrices $C_{\pm}$ and D respectively. These matrices are computed together with the LU factorizations of the influences matrices B and $C_{\pm}$.

(2) Obtention of the gradient of ϕ on the N-node mesh
  (i) If $S'\neq S$ one first obtain the normal flux $F=\nabla\phi\cdot\mathbf{n}$ on the whole mesh by solving (11) under the prescribed boundary conditions (2). One thus encounters a dense and $2N\times 2N$ square matrix for the generalized and discretized unknown $X=(\phi,\nabla\phi\cdot\mathbf{n})$ on S.
  (ii) Solve the discretized Eq. (37) to obtain the potential gradient $\nabla\phi=\phi_{,i}\mathbf{e}_i$ on the N-node mesh.

(3) Obtention of the cartesian derivatives $\phi_{i_1\ldots i_k}$ for $2\leqslant k\leqslant m$

We successively work out as k increases from 2 to m the following steps:
  (i) Compute $\nabla\phi_{i_1\ldots i_{k-1}}\cdot\mathbf{n}$ from the value of $\phi_{i_1\ldots i_{k-1}}$ by solving (35).
  (ii) Compute the gradient $\nabla\phi_{i_1\ldots i_{k-1}}=\phi_{i_1\ldots i_{k-1}i_k}\mathbf{e}_{i_k}$ on the given N-node mesh by solving (37).

Observe that we do not need derivatives of C or additional efforts as m increases for the advocated boostrapping scheme.

3. Case of a collection of connected solids

So far we only paid attention to the surface S of one connected solid. However, some encountered applications (for instance the analysis of particle–particle interactions

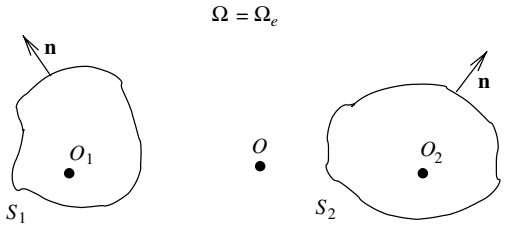

Fig. 3. Exterior problem for a multiply connected boundary S. Case of two surfaces S_1 and S_2, i.e. $L = 2$.

in our motivating problem of induced migration) involve several connected solids and one then faces with a boundary S consisting, as depicted in Fig. 3, of a finite number $L \geqslant 2$ of surfaces S_l, $l \in \{1,\ldots,L\}$ associated to connected solids Ω_l.

We equip each surface S_l with a N_l-node mesh, note $N = \sum_{l=1}^{L} N_l$ and assume that both $\mathbf{n}$ and the mean curvature C are given at each node of the total mesh on $S = \bigcup_{l=1}^{L} S_l$. The potential ϕ again fulfills the well-posed boundary value problem (2) and (3) for $\Omega_i = \mathbb{R}^3 \setminus \Omega_e$ and adequate additional conditions become:

$$\int_{S_l} F(\mathbf{y})\,\mathrm{d}S_l(\mathbf{y}) = 0 \quad \text{if } S_l \subset S' \text{ for interior problems.} \tag{38}$$

As the reader may easily check by proceeding as detailed in Section 2.1 for one connected solid boundary, the values of ϕ and its normal flux $\nabla\phi\cdot\mathbf{n}$ on the entire surface $S = \bigcup_{l=1}^{L} S_l$ again satisfy (11). Because for $\mathbf{x}$ on S_p we actually have

$$\int_{S_l} \frac{(\mathbf{x}-\mathbf{y})\cdot\mathbf{n}(\mathbf{y})}{|\mathbf{x}-\mathbf{y}|^3}\,\mathrm{d}S_l(\mathbf{y}) = 0 \quad \text{if } l \neq p, \tag{39}$$

this boundary-integral equation also reads

$$\begin{aligned} &-2\pi(1^{+}_{-}1)\phi(\mathbf{x}) + \int_{S_p} [\phi(\mathbf{y})-\phi(\mathbf{x})]\frac{(\mathbf{x}-\mathbf{y})\cdot\mathbf{n}(\mathbf{y})}{|\mathbf{x}-\mathbf{y}|^3}\,\mathrm{d}S_p(\mathbf{y}) \\ &\quad + \sum_{l\neq p}\int_{S_l} \phi(\mathbf{y})\frac{(\mathbf{x}-\mathbf{y})\cdot\mathbf{n}(\mathbf{y})}{|\mathbf{x}-\mathbf{y}|^3}\,\mathrm{d}S_l(\mathbf{y}) \\ &\quad = \int_S \frac{[\nabla\phi\cdot\mathbf{n}](\mathbf{y})}{|\mathbf{x}-\mathbf{y}|}\,\mathrm{d}S(\mathbf{y}) \quad \text{if } \mathbf{x}\in S_l. \end{aligned} \tag{40}$$

Taking into account the boundary conditions (2), one again arrives at a discretized linear system of $2N\times 2N$ dense influence matrix and $2N$ generalized unknown $X = (\phi, \nabla\phi\cdot\mathbf{n})$ on the given N-node mesh of the whole boundary S. Thus, we henceforth assume that $\nabla\phi\cdot\mathbf{n}$ has been determined at each node and two circumstances arise:

(1) Case of an interior problem

Because we know $\mathbf{n}$, C and $\nabla\phi\cdot\mathbf{n}$ on S_p we can immediately deduce, as advocated in Section 2, the cartesian derivatives of ϕ on the N_p-node mesh on each surface S_p. Since this procedure holds for any surface S_p it provides the required cartesian derivatives of ϕ on S.

(2) Case of an exterior problem

In such a case we cannot any more invoke the results established in Section 2 because the surface S is made of a collection of several surface S_l. The proposed procedure then consists in the following steps:

(i) *Step* 1: We first resort to a single-layer representation of ϕ in $\Omega\cup S$, i.e. we set

$$\phi(\mathbf{x}) = \sum_{l=1}^{L}\phi_l(\mathbf{x}), \quad \phi_l(\mathbf{x}) = \int_{S_l} q_l(\mathbf{y})\,\mathrm{d}S_l(\mathbf{y})/|\mathbf{x}-\mathbf{y}| \quad \text{for } \mathbf{x}\in\Omega\cup S. \tag{41}$$

From the knowledge of the normal flux $\nabla\phi\cdot\mathbf{n}$ on S, the introduced 'source' densities $q_1,\ldots,q_L$ are governed by the classical Fredholm boundary-integral equation of the second kind

$$\begin{aligned} &2\pi q_p(\mathbf{x}) + \int_{S_p}\frac{q_p(\mathbf{y})(\mathbf{x}-\mathbf{y})\cdot\mathbf{n}(\mathbf{x})}{|\mathbf{x}-\mathbf{y}|^3}\,\mathrm{d}S_p(\mathbf{y}) \\ &\quad + \sum_{l\neq p}\int_{S_l}\frac{q_l(\mathbf{y})(\mathbf{x}-\mathbf{y})\cdot\mathbf{n}(\mathbf{x})}{|\mathbf{x}-\mathbf{y}|^3}\,\mathrm{d}S_l(\mathbf{y}) = -[\nabla\phi\cdot\mathbf{n}](\mathbf{x}) \\ &\quad \text{for } \mathbf{x}\in S_p, \quad p\in\{=1,\ldots,L\}. \end{aligned} \tag{42}$$

Note that any integral occurring in (42) is regular. If the integral over S_p is denoted by $\mathscr{L}_p(\mathbf{x})$, the use for $\mathbf{x}$ on S_p of (6) indeed yields

$$\begin{aligned} \mathscr{L}_p(\mathbf{x}) = q_p(\mathbf{x})&\left\{\int_{S_p}\frac{(\mathbf{x}-\mathbf{y})\cdot[\mathbf{n}(\mathbf{x})-\mathbf{n}(\mathbf{y})]\,\mathrm{d}S_p(\mathbf{y})}{|\mathbf{x}-\mathbf{y}|^3} - 2\pi\right\} \\ &+ \int_{S_p}\frac{[q_p(\mathbf{y})-q_p(\mathbf{x})](\mathbf{x}-\mathbf{y})\cdot\mathbf{n}(\mathbf{x})\,\mathrm{d}S_p(\mathbf{y})}{|\mathbf{x}-\mathbf{y}|^3}. \end{aligned} \tag{43}$$

Eq. (42) is well-posed: as soon as $\nabla\phi\cdot\mathbf{n}\in H^{-1/2}(S)$ it admits a unique solution $(q_1,\ldots,q_L)$ in $H^{-1/2}(S)$ (see [12]). These unknown 'source' densities $q_1,\ldots,q_L$ may be efficiently and accurately obtained by resorting to iterative and/or fast multipole methods because the interaction between two different points $\mathbf{x}$ and $\mathbf{y}$ on S quickly decays (it exhibits the strong $1/|\mathbf{x}-\mathbf{y}|^2$-decay).

(ii) *Step* 2: When looking at the derivatives of ϕ on the surface S_p it is fruitful noting that our single-layer potential ϕ_p obeys

$$\begin{aligned} &\nabla^2\phi_p = 0 \quad \text{in } \Omega_p, \\ &[\nabla\phi_p]\cdot\mathbf{n} = F_p : [\nabla\phi\cdot\mathbf{n}] - \sum_{l\neq p}[\nabla\phi_l\cdot\mathbf{n}] \quad \text{on } S_p, \end{aligned} \tag{44}$$

$$|(O_pM)\phi_p| \leqslant \mathrm{O}(1) \quad \text{as } |O_pM|\to\infty, \tag{45}$$

where Ω_p denotes the unbounded domain outside S_p and, as indicated in Fig. 3, O_p designates a given point inside S_p. In other words, the potential ϕ_p obeys a well-posed exterior Neumann problem about the surface S_p. Moreover, it is straightforward to compute on the N_p-node mesh of S_p the normal flux F_p, introduced by (44), from the total normal flux $\nabla\phi\cdot\mathbf{n}$ and the previously obtained 'source' densities q_l, $l\neq p$. Accordingly, one immediately gains at each node on S_p the cartesian derivatives $\phi_{p,i_1\ldots i_m}$ of order $m\geqslant 1$ by applying the recursion scheme presented in Section 2.3 for each surface S_p. Finally, the cartesian deriva-

tives of the total potential are readily computed on the surface S_p from the link

$$[\phi_{,i_1\ldots i_m}](\mathbf{x}) = [\phi_{p,i_1\ldots i_m}](\mathbf{x}) + \sum_{l\neq p}\int_{S_l} q_l(\mathbf{y})\left[\frac{1}{|\mathbf{x}-\mathbf{y}|}\right]_{,i_1\ldots i_m} \mathrm{d}S_l(\mathbf{y}) \tag{46}$$

as soon as one notes that available recursion relations [17] easily provides the required cartesian derivatives of $1/|\mathbf{x}-\mathbf{y}|$, with respect to $\mathbf{x}$, at any desired order.

4. Numerical implementation and illustrating benchmarks

In order to test the efficiency of the procedure proposed in Sections 2 and 3 for one or several connected solid(s) respectively, we present in this section a numerical implementation and a few illustrating and carefully selected benchmarks against analytical and available solutions.

4.1. Numerical method

For simplicity the normal flux $F = \nabla\phi\cdot\mathbf{n}$ is prescribed on the surface, i.e. $S' = S$ in (2) (if this is not the case, one has only to invert the additional integral Eqs. (11) or (40) by the technique described below). Thus, we need to compute the integrals $I_l(\mathbf{x}, S)$ or $I_l(\mathbf{x}, S_l)$ and to invert the boundary-integral Eqs. (16) (or (37)), (35) and (42) that all adopt the form $MX = Y$ with X unknown and a right-hand side Y to be accurately evaluated. As previously mentioned, we implemented a collocation point Boundary Element Method although a Galerkin method may be also employed. Since details are available in any standard textbooks (see, among others, [18–20]), we only briefly present the main steps of the procedure.

Step 1: Henceforth, we choose $L \geqslant 1$ with $L = 1$ for one connected solid with surface $S = S_1$. The N_l-node mesh on S_l consists of $N_e(l)$ 6-node triangular elements $\Delta_l^{(e)}$, with $1 \leqslant e \leqslant N_e(l)$, which are mapped to the standard triangle Δ of inequations $0 \leqslant \xi_1 \leqslant 1$, $0 \leqslant \xi_2 \leqslant 1$ and $\xi_1 + \xi_2 \leqslant 1$ in plane cartesian and intrinsic coordinates $\boldsymbol{\xi} = (\xi_1, \xi_2)$ by six bilinear shape functions λ_m such that

$$\lambda_1(\boldsymbol{\xi}) = (2\xi_3 - 1)\xi_3, \quad \lambda_2(\boldsymbol{\xi}) = 4\xi_1\xi_3, \quad \lambda_3(\boldsymbol{\xi}) = (2\xi_1 - 1)\xi_1, \tag{47}$$

$$\lambda_4(\boldsymbol{\xi}) = 4\xi_1\xi_2, \quad \lambda_5(\boldsymbol{\xi}) = (2\xi_2 - 1)\xi_2, \quad \lambda_6(\boldsymbol{\xi}) = 4\xi_2\xi_3, \tag{48}$$

if one sets $\xi_3 = 1 - \xi_1 - \xi_2$. Any function g on S is interpolated on the element $\Delta_l^{(e)}$, of nodal points $\mathbf{y}_l^{(e,m)}$ with $m \in \{1,\ldots,6\}$, by using the same shape functions. Hence,

$$g(\mathbf{y}) = \sum_{m=1}^{6}\lambda_m(\xi)g_l^{(e,m)} \quad \text{for } \mathbf{y} = \mathbf{y}(\xi) = \sum_{m=1}^{6}\lambda_m(\xi)\mathbf{y}_l^{(e,m)} \tag{49}$$

if $g_l^{(e,m)}$ designates the value of g at the node $\mathbf{y}_l^{(e,m)}$ of S_l and one thus builds a continuous and isoparametric interpolation of g on the whole surface S which is quite suitable because we assume that g is $C^{0,\alpha}$, i.e. $|g(\mathbf{y}) - g(\mathbf{x})| < C_g|\mathbf{y}-\mathbf{x}|^\alpha$ for $\mathbf{x}$, $\mathbf{y}$ on S and $C_g > 0$, $\alpha > 0$.

Step 2: Any encountered weakly singular integral is of the following form

$$R_1(\mathbf{x}) = \int_{S_l}\frac{g(\mathbf{y})}{|\mathbf{x}-\mathbf{y}|}\,\mathrm{d}S_l(\mathbf{y}),$$
$$R_2^i(\mathbf{x}) = \int_{S_l}\frac{[g(\mathbf{x}) - g(\mathbf{y})](\mathbf{x}-\mathbf{y})\cdot\mathbf{a}}{|\mathbf{x}-\mathbf{y}|^3}\,\mathrm{d}S_l(\mathbf{y}) \tag{50}$$

with $\mathbf{a} = \mathbf{e}_i$ or $\mathbf{a} \in \{\mathbf{n}(\mathbf{x}), \mathbf{n}(\mathbf{y})\}$ and we exploit the decomposition

$$\int_{S_l} f(\mathbf{x},\mathbf{y})\,\mathrm{d}S_l(\mathbf{y}) = \sum_{e=1}^{N_e(l)} I_l^{(e)}(\mathbf{x}),$$
$$I_l^{(e)}(\mathbf{x}) = \int_{\Delta_l^{(e)}} f(\mathbf{x},\boldsymbol{\xi})J(\boldsymbol{\xi})\,\mathrm{d}\boldsymbol{\xi}, \tag{51}$$

where J designates the Jacobian of the mapping of our cartesian coordinates $\mathbf{y}$ to the triangular coordinates $\boldsymbol{\xi}$. Each integral $I_l^{(e)}(\mathbf{x})$ is accurately computed as indicated in [21] if $\mathbf{x}$ does not lie on the element $\Delta_l^{(e)}$ and by analytical removal of the $1/|\mathbf{x}-\mathbf{y}|$-type weakly singular behavior via polar coordinates centered at $\mathbf{x}$ in the space of intrinsic coordinates $\boldsymbol{\xi}$ otherwise. Hence, one only faces with regular integrations which are numerically performed by standard Gaussian integrations formulas (see, for instance, [22]).

Step 3: Under the treatment of steps 1 and 2, each boundary-integral equation becomes a discretized matrix system of N, $2N$ or $3N$ unknown for Eqs. (35), (42) and (37). The solution is obtained by using a LU factorization algorithm (subroutines DGETRF and DGETRS of the Lapack Library) for any illustrating example ($L \leqslant 3$) but (42) should be adequately solved by an iterative methods as soon as L becomes large (roughly exceeding 10).

4.2. Numerical benchmarks

The previous numerical implementation holds for smooth enough but arbitrarily shaped surfaces S_l (one only needs an analytical description of S_l that exactly gives the required unit normal $\mathbf{n}$ and mean curvature C). For each retained illustrating example S_l is the surface of an ellipsoid of semi-axis $a_1(l)$, $a_2(l)$, $a_3(l)$ which is 'centered' at the point O_l (see Fig. 3 for $L = 2$) of cartesian coordinates $x_i(l) = \mathbf{OO}_l\cdot\mathbf{e}_i$. For any point $\mathbf{x} = x_i\mathbf{e}_i$ of S_l if we set $\bar{x}_i = x_i - x_i(l)$ it follows that (without summation over i in (52))

$$\frac{\bar{x}_1^2}{a_1^2(l)} + \frac{\bar{x}_2^2}{a_2^2(l)} + \frac{\bar{x}_3^2}{a_3^2(l)} = 1, \quad \mathbf{n}(\mathbf{x})\cdot\mathbf{e}_i = \frac{s(\mathbf{x})\bar{x}_i}{a_i^2(l)},$$
$$s^{-2}(\mathbf{x}) = \frac{\bar{x}_1^2}{a_1^4(l)} + \frac{\bar{x}_2^2}{a_2^4(l)} + \frac{\bar{x}_3^2}{a_3^4(l)}, \tag{52}$$

$$C(\mathbf{x}) = [\nabla\cdot\mathbf{n}](\mathbf{x}) = s(\mathbf{x})\left\{\frac{1}{a_1^2(l)} + \frac{1}{a_2^2(l)} + \frac{1}{a_3^2(l)} - s^2(\mathbf{x})\left[\frac{\bar{x}_1^2}{a_1^6(l)} + \frac{\bar{x}_2^2}{a_2^6(l)} + \frac{\bar{x}_3^2}{a_3^6(l)}\right]\right\}. \tag{53}$$

In order to define the N_l-node mesh on S_l we introduce the elliptical angles $\theta_l \in [0, 2\pi]$ and $\varphi_l \in [0, \pi]$ such that

$$\bar{x}_1 = a_1(l)\sin\varphi_l\cos\theta_l, \quad \bar{x}_2 = a_2(l)\sin\varphi_l\sin\theta_l,$$
$$\bar{x}_3 = a_3(l)\cos\varphi_l \quad \text{for } \bar{x}_i = x_i - x_i(l) \tag{54}$$

and locate each point of S_l by its angles (θ_l, φ_l). Under these notations, the N_l-node mesh is characterized by two positive integers $N_\varphi(l) \geqslant 3$, $E(l) \geqslant 0$ and consists of the points $\mathbf{x} = (\theta_l, \varphi_l)$ such that

$$\theta_l = 2\pi(n_\theta - 1)/N_\theta(l), \quad \varphi_l = \pi n_\varphi/[2N_\varphi(l)],$$
$$N_\theta(l) = 12 \times 2^{E(l)} \tag{55}$$

for positive integers n_θ and n_φ that obey the conditions

$$1 \leqslant n_\theta \leqslant N_\theta(l) \quad \text{if } 2 \leqslant n_\varphi \leqslant 2[N_\varphi(l) - 1], \tag{56}$$
$$n_\theta = 2k \quad \text{with } k \in \{0, \ldots, N_\theta(l)/2 - 1\} \text{ if } n_\varphi \in \{1, 2N_\varphi(l) - 1\}. \tag{57}$$

Accordingly, the pair $(N_\varphi(l), E(l))$ defines a N_l-node mesh of $N_e(l)$ boundary elements on S_l with

$$N_l = 2\{1 + N_\theta(l)[N_\varphi(l) - 1]\},$$
$$N_e(l) = N_\theta(l)[N_\varphi(l) - 1], \quad N_\theta(l) = 12 \times 2^{E(l)} \tag{58}$$

and for convenience we shall note $N_l = [N_\varphi(l), E(l)]$.

4.2.1. Case of the surface S of one connected solid: L = 1

We spread $N = N_1 = [N_\varphi(1), E(1)]$ nodal points $M(n)$, with $n \in \{1, \ldots, N\}$, on S and consider both interior and exterior illustrating potential problems. If g and g_{num} respectively denote the exact and computed values of g at the point M on S the employed numerical error $\langle g \rangle$ is the relative l^∞-norm of the error defined as

$$\langle g \rangle : \frac{\text{Max}_{(n=1,\ldots,N)}|g(M(n)) - g_{\text{num}}(M(n))|}{|g|}$$
$$\text{if } |g| : \text{Max}_{(M \text{ on } S)}|g(M)| \neq 0, \tag{59}$$
$$\langle g \rangle : \text{Max}_{(n=1,\ldots,N)}|g_{\text{num}}(M(n))| \quad \text{if } g = 0 \text{ on } S. \tag{60}$$

Note that the selected relative error $\langle g \rangle$ provides a clear indication of the incurred local error at each point of the boundary S. In addition, one readily needs to evaluate for each addressed numerical benchmark the l^∞-norm $|g|$ of $g = \phi_{,i}$ and $g = \phi_{,ij}$. Whenever possible this is analytically achieved. In other cases, one locates any point M on S by its angles θ and φ, as introduced in (54), and it has been possible to obtain in closed form each partial derivative $G_{,\theta} := \partial G/\partial\theta$ and $G_{,\varphi} := \partial G/\partial\varphi$ of the function $G(\theta, \varphi) = g(M)$. The requested quantity $|g|$ is then numerically obtained by iteratively enforcing to zero those derivatives $G_{,\theta}$ and $G_{,\varphi}$ through a two-dimensional Newton–Raphson algorithm whose suitable guess value (θ_g, φ_g) is guided by the evaluation of $|G(\theta, \varphi)|$ on a fine grid in the domain $[0, 2\pi] \times [0, \pi]$.

Besides the errors $\langle g \rangle$ it is worth calculating the order of convergence α with respect to $N^{-1/2}$ with N the number of collocation points. For errors $\langle g \rangle'$ and $\langle g \rangle''$ associated with N' and N'', respectively the number α is computed as follows:

$$\alpha = -2\log(\langle g \rangle''/\langle g \rangle')/\log(N''/N'). \tag{61}$$

(1) Potential problems for a sphere.

The following problems are addressed for the unit sphere $S = \{\mathbf{x}, r = 1\}$ for $N' = [4, 0] = 74$, $N'' = [6, 1] = 242$ or $N''' = [12, 2] = 1058$ collocation points and a prescribed normal flux $\nabla\phi \cdot \mathbf{n}$:

(a) The interior potential $\phi = x_1x_2x_3$ with $\nabla\phi \cdot \mathbf{n} = 3x_1x_2x_3$. For this potential note that $|\phi_{,ii}| = 0$.
(b) The exterior case of $\nabla\phi \cdot \mathbf{n} = \mathbf{n} \cdot \mathbf{e}_2$ which admits the exact solution $\phi = -x_2/[2r^3]$ outside the unit sphere (for $r = |\mathbf{x}| \geqslant 1$).

The associated values of the l^∞-norm $|g|$ are given in Appendix B. As indicated in Table 1, the computed cartesian derivatives exhibit a nice convergence towards the exact values as the number N of collocation

Table 1
Numerical errors and order of convergence α with respect to $N^{-1/2}$ for first- and second-order cartesian derivatives of potentials at the surface S of a unit sphere

$\langle g \rangle$; α	(a), N'	(a), N''	(a), N'''	(b), N'	(b), N''	(b), N'''
$\langle \phi_{,1} \rangle$; α	0.274987	0.054851; 2.9	0.005940; 3.2	0.070757	0.012800; 3.1	0.001747; 2.9
$\langle \phi_{,2} \rangle$; α	0.204884	0.054851; 2.4	0.005940; 3.2	0.065337	0.012127; 3.1	0.001402; 3.1
$\langle \phi_{,3} \rangle$; α	0.200368	0.056076; 2.3	0.007365; 2.9	0.048747	0.013753; 2.3	0.001956; 2.8
$\langle \phi_{,11} \rangle$; α	0.175995	0.060885; 1.9	0.013007; 2.2	0.188937	0.035614; 3.1	0.004741; 2.9
$\langle \phi_{,12} \rangle$; α	0.097378	0.050092; 1.2	0.010822; 2.2	0.108113	0.034426; 2.1	0.004637; 2.9
$\langle \phi_{,13} \rangle$; α	0.096749	0.065197; 0.7	0.010228; 2.7	0.156295	0.046441; 2.2	0.005984; 3.0
$\langle \phi_{,21} \rangle$; α	0.137258	0.050092; 1.8	0.010822; 2.2	0.108325	0.028433; 2.4	0.003747; 2.9
$\langle \phi_{,22} \rangle$; α	0.132980	0.065197; 1.3	0.013007; 2.3	0.164448	0.035501; 2.8	0.004992; 2.8
$\langle \phi_{,23} \rangle$; α	0.141025	0.065197; 1.4	0.010228; 2.7	0.124870	0.029341; 2.6	0.005427; 2.4
$\langle \phi_{,31} \rangle$; α	0.140420	0.063853; 1.4	0.011034; 2.5	0.142334	0.038800; 2.4	0.005837; 2.7
$\langle \phi_{,32} \rangle$; α	0.182878	0.063853; 1.9	0.011034; 2.5	0.129976	0.026091; 2.9	0.003593; 2.9
$\langle \phi_{,33} \rangle$; α	0.194082	0.072146; 1.8	0.016348; 2.1	0.100155	0.027197; 2.4	0.004833; 2.5

Labels (a) and (b) indicate results for selected interior and exterior problems (a) and (b), respectively whereas $N' = [4, 0] = 74$, $N'' = [6, 1] = 242$ and $N''' = [12, 2] = 1058$. The associated values of the l^∞-norm $|g|$ are given in Appendix B, Table 5.

Table 2
Numerical errors and order of convergence α with respect to $N^{-1/2}$ for first- and second-order cartesian derivatives of potentials at the surface S of the ellipsoid $a_1(1) = 1$, $a_2(1) = 0.8$ and $a_1(3) = 1.5$

$\langle g \rangle$; α	(c), N'	(c), N''	(c), N'''	(d), N'	(d), N''	(d), N'''
$\langle \phi_{,1} \rangle$; α	0.105198	0.018826; 3.1	0.003137; 3.3	0.026527	0.008327; 2.1	0.001547; 3.1
$\langle \phi_{,2} \rangle$; α	0.066638	0.015554; 2.6	0.002279; 3.5	0.054597	0.008941; 3.3	0.002462; 2.3
$\langle \phi_{,3} \rangle$; α	0.129888	0.029200; 2.7	0.006766; 2.7	0.043300	0.011882; 2.4	0.003033; 2.5
$\langle \phi_{,11} \rangle$; α	0.122808	0.048079; 1.7	0.012803; 2.4	0.086126	0.022115; 2.5	0.005112; 2.7
$\langle \phi_{,12} \rangle$; α	0.048284	0.022823; 1.4	0.005045; 2.7	0.083069	0.048693; 1.0	0.008662; 3.1
$\langle \phi_{,13} \rangle$; α	0.137843	0.051232; 1.8	0.013070; 2.5	0.076200	0.032966; 1.5	0.006300; 3.0
$\langle \phi_{,21} \rangle$; α	0.067429	0.024450; 1.8	0.005320; 2.8	0.085134	0.021584; 2.5	0.004835; 2.7
$\langle \phi_{,22} \rangle$; α	0.178981	0.082386; 1.4	0.022547; 2.4	0.193129	0.031528; 3.3	0.009793; 2.1
$\langle \phi_{,23} \rangle$; α	0.118376	0.039800; 2.0	0.010852; 2.4	0.147535	0.027247; 3.1	0.005894; 2.8
$\langle \phi_{,31} \rangle$; α	0.162265	0.051109; 2.1	0.015254; 2.2	0.093894	0.039016; 1.6	0.011319; 2.3
$\langle \phi_{,32} \rangle$; α	0.107586	0.035236; 2.0	0.011034; 2.1	0.156953	0.048854; 2.1	0.012648; 2.5
$\langle \phi_{,33} \rangle$; α	0.084732	0.024246; 2.3	0.008030; 2.0	0.168433	0.029058; 3.2	0.011048; 1.8

Labels (c) and (d) indicate results for selected interior and exterior problems (c) and (d), respectively whereas $N' = [8,0] = 170$, $N'' = [12,1] = 530$ and $N''' = [18,2] = 1634$. The associated values of the l^∞-norm $|g|$ are given in Appendix B, Table 5.

points increases both for the interior and the exterior potentials. The refined 1058-node mesh provides accurate enough results for any further surface integration on S, as needed for our motivating integrals I_1 and I_2 (see definitions (1)).

(2) Potential problems for an ellipsoid.

We take $O_1 = O$, $a_1(1) = a = 1$, $a_2(1) = b = 0.8$, $a_3(1) = c = 1.5$ and successively employ $N' = [8,0] = 170$, $N'' = [12,1] = 530$ and $N''' = [18,2] = 1634$ nodal points for the following potential problems:

(c) The interior potential $\phi = x_1x_2x_3$ with $\nabla\phi \cdot \mathbf{n} = s(\mathbf{x})x_1x_2x_3[a^{-2} + b^{-2} + c^{-2}]$.
(d) The exterior potential $\phi(\mathbf{x}) = 1/[2r]$ for $r = |\mathbf{x}|$.

Again, we provide the associated values of the l^∞-norm $|g|$ in Appendix B. As revealed by Table 2, we still obtain excellent agreement between the computed and exact cartesian derivatives on the surface of the ellipsoid both for interior and exterior cases (c) and (d). Note that we spread a bit more nodal points on our somewhat 'slender' ellipsoid than

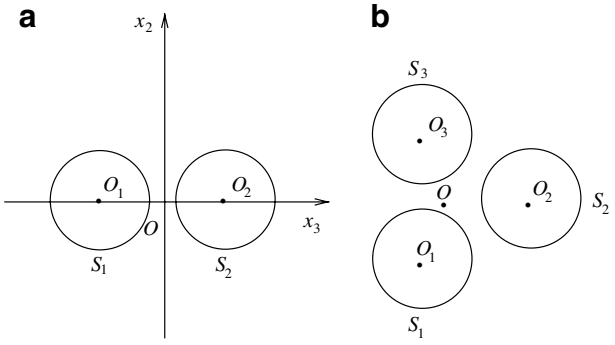

Fig. 4. (a) Side view of the 2-sphere cluster with $\mathbf{O_1O_2} = 2d\mathbf{e_3}$ and $d > 1$. (b) Top view, in the x_1–x_2 plane, of the 3-sphere cluster.

Table 3
Numerical errors $\langle g \rangle_1 = \langle g \rangle_2$ and order of convergence α with respect to $N^{-1/2}$ of first- and second-order cartesian derivatives of the exterior potential at the multiply connected surface $S_1 \cup S_2$ of a 2-sphere cluster versus the number $N_1 = N_2$ of nodal points on S_1 and S_2 for two center-to-center distances $2d$

$\langle g \rangle_i$; α	(i), N'	(i), N''	(i), N'''	(ii), N'	(ii), N''	(ii), N'''
$\langle \phi_{,1} \rangle_i$; α	0.015711	0.001822; 3.9	0.000154; 3.6	0.015023	0.001746; 3.9	0.000153; 3.5
$\langle \phi_{,2} \rangle_i$; α	0.014815	0.001822; 3.9	0.000154; 3.6	0.016498	0.001746; 3.9	0.000153; 3.5
$\langle \phi_{,3} \rangle_i$; α	0.019907	0.001985; 4.2	0.000069; 4.9	0.019071	0.001903; 4.2	0.000067; 4.8
$\langle \phi_{,11} \rangle_i$; α	0.066927	0.012555; 3.0	0.001440; 3.1	0.067904	0.012615; 3.1	0.001449; 3.1
$\langle \phi_{,12} \rangle_i$; α	0.046019	0.012898; 2.3	0.001772; 2.9	0.046119	0.012739; 2.3	0.001762; 2.9
$\langle \phi_{,13} \rangle_i$; α	0.046977	0.013973; 2.2	0.001982; 2.8	0.045661	0.013719; 2.2	0.001956; 2.8
$\langle \phi_{,21} \rangle_i$; α	0.073424	0.012898; 3.1	0.001772; 2.9	0.073505	0.013041; 3.1	0.001762; 2.9
$\langle \phi_{,22} \rangle_i$; α	0.133780	0.024611; 3.1	0.002824; 3.1	0.069302	0.012615; 3.1	0.001449; 3.1
$\langle \phi_{,23} \rangle_i$; α	0.051481	0.013947; 2.4	0.001982; 2.8	0.050085	0.013719; 2.4	0.001956; 2.8
$\langle \phi_{,31} \rangle_i$; α	0.042023	0.005985; 3.5	0.000610; 3.3	0.045403	0.005809; 3.7	0.000600; 3.3
$\langle \phi_{,32} \rangle_i$; α	0.036623	0.005985; 3.5	0.000610; 3.3	0.039540	0.005809; 3.5	0.000600; 3.3
$\langle \phi_{,33} \rangle_i$; α	0.058510	0.009314; 3.3	0.000752; 3.6	0.047658	0.008212; 3.2	0.000761; 3.4

(i) case $d = 2$. (ii) case $d = 1.2$. Here we have $N' = [4,0] = 74$, $N'' = [6,1] = 242$ and $N''' = [12,2] = 1058$.

on the unit sphere in order to gain computed results of comparable accuracy.

4.2.2. Case of the surface S of a collection of connected solids: $L \geqslant 2$

Since any interior case actually reduces to interior problems for the simply connected surfaces S_l we restrict our benchmarks to exterior potentials. The numerical error $\langle g \rangle_l$ on S_l for a function g defined on the whole surface S is given as defined in (59) and (60) where one replaces the surface S with the surface S_l of the considered sphere. The value of each l^∞-norm $|g|$ is computed as mentioned in Section 4.2.1.

(1) Case of a 2-sphere cluster.
We consider, as depicted in Fig. 4(a), two unit spheres S_1 and S_2 centered at O_1 and O_2 respectively with $\mathbf{O_1O_2} = 2d\mathbf{e}_3$ and $d > 1$. The exterior potential is $\phi(M) = 1/O_1M + 1/O_2M$ and its normal flux is prescribed on $S = S_1 \cup S_2$. For symmetry reasons $\langle g \rangle_1 = \langle g \rangle_2$ for $g = \phi_{,i}$ and $g = \phi_{,ij}$. These errors are given in Table 3 if $d = 2$ or $d = 1.2$ (close spheres) for three numbers ($N_l = 74{,}242$ or 1058) of collocation points on the spheres. Clearly, computed results are in excellent agreement with theoretical ones both for moderate ($d = 2.0$) and small ($d = 1.2$) gaps between the spheres. If the numerical errors are comparable for these two center-to-center distances one of course expects a loss of accuracy for near-touching spheres (as $d \to 1$) because the approximation of the integral on the right-hand side of (46) deriorates as $d - 1$ vanishes.

(2) Case of a 3-sphere cluster.
Finally, we consider a 3-sphere cluster with centers of the spheres in the $x_1 - x_2$ plane and located at the vertices of an equilateral triangle, as sketched in Fig. 4(b). Again, the center-to-center distance is denoted by $2d$ and each sphere has unit radius so that $d > 1$. More precisely, we set

$$x_1(l) = \frac{2d\cos(\alpha_l)}{\sqrt{3}}, \quad x_2(l) = \frac{2d\sin(\alpha_l)}{\sqrt{3}},$$
$$\alpha_l = \frac{2\pi}{3}(l+1) \quad \text{with } l = 1, 2, 3. \tag{62}$$

The exact potential is $\phi(M) = 1/O_1M + 1/O_2M + 1/O_3M$ and we confine ourselves to the severe benchmark $d = 1.2$, a case of very close spheres. For symmetry reasons note that $\langle g \rangle_1 = \langle g \rangle_3$. As shown in Table 4, the computed errors for the cartesian derivatives vanish as the number of collocation points on each sphere increases.

5. Concluding remarks

In summary, a new procedure has been both proposed and numerically worked out and tested for the accurate approximation of the cartesian derivatives of potentials on a simply or multiply connected surface. The advocated recursion scheme appeals to the same and very few boundary-integral equations and geometrical informations on the geometry (the normal vector and the mean curvature) whatever the order of the required derivatives. These pleasant features make it possible to successively compute, if necessary, higher and higher order derivatives at a reasonable cpu cost. Exterior problems for a multiply connected surface consisting of a large number of simply connected boundaries may be easily addressed by using iterative methods for the integral-equations bearing on the whole surface. Finally, let us note that the proposed approach is likely to apply to the Helmholtz equation and linear elasticity in 3D problems. Such challenging tasks are under current investigation.

Appendix A

This Appendix both establishes (29) and proves that $A_i^{0,\epsilon}(\mathbf{x}), A_i^{1,\epsilon}(\mathbf{x})$ and $P_{ij}^{\epsilon}(\mathbf{x})$ vanish as ϵ goes to zero. The

Table 4
Numerical errors $\langle g \rangle_l$ and order of convergence α with respect to $N^{-1/2}$ for first- and second-order cartesian derivatives of the exterior potential at the multiply connected surface $S_1 \cup S_2 \cup S_3$ of a 3-sphere cluster with $d = 1.2$

$\langle g \rangle_l$; α	(a), $l = 1$	(b), $l = 1$	(c), $l = 1$	(a), $l = 2$	(b), $l = 2$	(c), $l = 2$
$\langle \phi_{,1} \rangle_l$; α	0.013926	0.001616; 3.9	0.000155; 3.4	0.013622	0.001587; 3.9	0.000152; 3.4
$\langle \phi_{,2} \rangle_l$; α	0.012897	0.001583; 3.8	0.000155; 3.4	0.015101	0.001781; 3.9	0.000151; 3.6
$\langle \phi_{,3} \rangle_l$; α	0.019566	0.001926; 4.2	0.000092; 4.4	0.019566	0.001926; 4.2	0.000092; 4.4
$\langle \phi_{,11} \rangle_l$; α	0.066649	0.012515; 3.0	0.001422; 3.1	0.061909	0.011988; 3.0	0.001389; 3.1
$\langle \phi_{,12} \rangle_l$; α	0.041147	0.011338; 2.3	0.001562; 2.9	0.041083	0.011207; 2.4	0.001544; 2.9
$\langle \phi_{,13} \rangle_l$; α	0.048032	0.013777; 2.3	0.001956; 2.8	0.046054	0.013565; 2.3	0.001937; 2.8
$\langle \phi_{,21} \rangle_l$; α	0.065806	0.011364; 3.2	0.001564; 2.9	0.066016	0.011174; 3.2	0.001540; 2.9
$\langle \phi_{,22} \rangle_l$; α	0.053278	0.009965; 3.1	0.001169; 3.1	0.070187	0.013061; 3.1	0.001490; 3.1
$\langle \phi_{,23} \rangle_l$; α	0.049833	0.013597; 2.4	0.001944; 2.8	0.050648	0.014101; 2.3	0.001985; 2.8
$\langle \phi_{,31} \rangle_l$; α	0.040017	0.005855; 3.5	0.000609; 3.3	0.039937	0.005729; 3.5	0.000596; 3.3
$\langle \phi_{,32} \rangle_l$; α	0.032362	0.005774; 3.1	0.000602; 3.3	0.033735	0.005939; 3.2	0.000619; 3.3
$\langle \phi_{,33} \rangle_l$; α	0.062707	0.009768; 3.4	0.000818; 3.6	0.062706	0.009768; 3.4	0.000818; 3.6

(a) case $N_1 = [4, 0] = 74$. (b) case $N_l = [6, 1] = 242$. (c) case $N_l = [12, 2] = 1058$.

starting point is the usual Stokes' theorem that gives, for any vector $\mathbf{u}$ defined and smooth enough in a neighborhood of S,

$$\int_{S(\epsilon)} \mathbf{rot}(\mathbf{u})\cdot\mathbf{n}\,\mathrm{d}S(\mathbf{y}) = \oint_{c_\epsilon} \mathbf{u}\cdot\mathbf{t}\,\mathrm{d}s(\mathbf{y}), \tag{63}$$

where the tangential and unit vector $\mathbf{t}$ is defined as introduced right after (28) and $\mathrm{d}s$ denotes the differential arc length on the closed path c_ϵ. From (63) it is possible to obtain, if $C := \nabla\cdot\mathbf{n}$ on the smooth enough boundary $S(\epsilon)$ and $\mathbf{v} = \mathbf{t}\wedge\mathbf{n}$, the identities

$$\int_{S(\epsilon)} [D_{ij}g](\mathbf{y})\,\mathrm{d}S(\mathbf{y}) = \oint_{c_\epsilon} g(\mathbf{e}_i\wedge\mathbf{e}_j)\cdot\mathbf{t}\,\mathrm{d}s(\mathbf{y}), \tag{64}$$

$$\int_{S(\epsilon)} g_{,i}(\mathbf{y})\,\mathrm{d}S(\mathbf{y}) = \int_{S(\epsilon)} [Cg + \nabla g\cdot\mathbf{n}][\mathbf{n}\cdot\mathbf{e}_i]\,\mathrm{d}S(\mathbf{y}) + \oint_{c_\epsilon} g\mathbf{v}\cdot\mathbf{e}_i\,\mathrm{d}s(\mathbf{y}). \tag{65}$$

In establishing the above results it is fruitful reminding (see [23, p. 1081 and 1084]) the usual identities

$$\begin{aligned} &(\mathbf{a}\wedge\mathbf{b})\wedge\mathbf{c} = (\mathbf{a}\cdot\mathbf{c})\mathbf{b} - (\mathbf{b}\cdot\mathbf{c})\mathbf{a},\\ &\mathbf{rot}(\mathbf{a}\wedge\mathbf{b}) = (\nabla\cdot\mathbf{b})\mathbf{a} - (\nabla\cdot\mathbf{a})\mathbf{b} + (\mathbf{b}.\nabla)\mathbf{a} - (\mathbf{a}.\nabla)\mathbf{b}. \end{aligned} \tag{66}$$

Accordingly, the definition (14) becomes

$$\begin{aligned} D_{ij}g &= (\mathbf{e}_i\wedge\mathbf{e}_j)\cdot(\mathbf{n}\wedge\nabla g) = [\nabla g\wedge(\mathbf{e}_i\wedge\mathbf{e}_j)]\cdot\mathbf{n}\\ &= \mathbf{rot}[g(\mathbf{e}_i\wedge\mathbf{e}_j)]\cdot\mathbf{n} \end{aligned} \tag{67}$$

and using (63) we obtain (64). Selecting $\mathbf{a} = \mathbf{n}$ and $\mathbf{b} = g\mathbf{e}_i$ in applying (66) and taking into account the definition of C and the property $\mathbf{n}_{,i}\cdot\mathbf{n} = 0$, the reader may also easily check that

$$[\mathbf{rot}(\mathbf{n}\wedge g\mathbf{e}_i)]\cdot\mathbf{n} = g_{,i} - [Cg + \nabla g\cdot\mathbf{n}]\mathbf{e}_i\cdot\mathbf{n}. \tag{68}$$

The use of (63) in conjunction with (68) then provides (65). Because $4\pi G(\mathbf{x},\mathbf{y}) = \rho^{-1}$ with $\rho = |\mathbf{x}-\mathbf{y}|$ a straightforward application of (65) for $g = \rho^{-1}$ then proves (29). In addition, from (64) and our definitions (14) of D_{ij}, (26) of F and (30)–(32) one obtains

$$\begin{aligned} &A_i^{0,\epsilon}(\mathbf{x}) = -\oint_{c_\epsilon}\left(\frac{1}{\rho}\right)_{,j} f(\mathbf{e}_i\wedge\mathbf{e}_j)\cdot\mathbf{t}\,\mathrm{d}s(\mathbf{y}),\\ &f = \mathrm{O}(\rho^{1+\alpha}) \quad \text{with } \alpha > 0, \quad \mathrm{d}s = \mathrm{O}(\rho), \end{aligned} \tag{69}$$

$$A_i^{1,\epsilon}(\mathbf{x}) = \int_{d(\epsilon)} [n_j(\mathbf{y}) - n_j(\mathbf{x})]\left(\frac{1}{\rho}\right)_{,j}\mathrm{d}S(\mathbf{y}) + n_j(\mathbf{x})\left[\int_{d(\epsilon)}\left(\frac{1}{\rho}\right)_{,j}\mathrm{d}S(\mathbf{y}) + \oint_{c_\epsilon}\frac{\mathbf{e}_j\cdot\mathbf{v}\,\mathrm{d}s(\mathbf{y})}{\rho}\right], \tag{70}$$

$$P_{ij}^{\epsilon}(\mathbf{x}) = \oint_{c_\epsilon}[(n_j(\mathbf{x}) - n_j(\mathbf{y}))\mathbf{e}_i - (n_i(\mathbf{x}) - n_i(\mathbf{y}))\mathbf{e}_j].\frac{\mathbf{v}\,\mathrm{d}s(\mathbf{y})}{\rho} + \oint_{c_\epsilon}\{(\mathbf{e}_i\wedge\mathbf{e}_j)\cdot\mathbf{t} + [n_j(\mathbf{y})\mathbf{e}_i - n_i(\mathbf{y})\mathbf{e}_j]\cdot\mathbf{v}\}\frac{\mathrm{d}s(\mathbf{y})}{\rho}. \tag{71}$$

In view of (69), that takes into account our property (15), $A_i^{0,\epsilon}(\mathbf{x})$ clearly vanishes with ϵ. For our smooth boundary S the first integral on the right-hand sides of (70) and (71) also collapses with ϵ. Because $[n_j(\mathbf{y})\mathbf{e}_i - n_i(\mathbf{y})\mathbf{e}_j]\cdot\mathbf{v} = (\mathbf{e}_i\wedge\mathbf{e}_j)\cdot(\mathbf{v}\wedge\mathbf{n})$ and $\mathbf{t} = \mathbf{n}\wedge\mathbf{v}$ the quantity $P_{ij}^{\epsilon}(\mathbf{x})$ thus tends to zero with ϵ. Finally, we consider the last term arising in (70), further denoted by $n_j(\mathbf{x})K_j(\mathbf{x})$. The integral over $d(\epsilon)$ in $K_j(\mathbf{x})$ is treated by using (65) and carefully taking care of the orientation of the tangential vector $\mathbf{t}$. One thus arrives at

$$\begin{aligned} K_j(\mathbf{x}) &= \int_{d(\epsilon)}\left(\frac{1}{\rho}\right)_{,j}\mathrm{d}S(\mathbf{y}) + \oint_{c_\epsilon}\frac{\mathbf{e}_j\cdot\mathbf{v}\,\mathrm{d}s(\mathbf{y})}{\rho}\\ &= \int_{d(\epsilon)}\left\{\left[\frac{Cn_j}{\rho}\right](\mathbf{y}) + \left[\nabla\left(\frac{1}{\rho}\right)\cdot\mathbf{n}\right](\mathbf{y})[n_j(\mathbf{y}) - n_j(\mathbf{x})] + n_j(\mathbf{x})\left[\nabla\left(\frac{1}{\rho}\right)\cdot\mathbf{n}\right](\mathbf{y})\right\}\mathrm{d}S(\mathbf{y}). \end{aligned} \tag{72}$$

Clearly, the integral over $d(\epsilon)$ in (72) vanishes with ϵ and this closes the proof.

Appendix B

Computed values of the l^∞-norms $|\phi_{,i}|$ and $|\phi_{,ij}|$ either for one connected solid (Table 5) and a collection of connected solids (Table 6). These values are obtained either analytically or numerically as detailed in Section 4.2.1.

Table 5
Computed values of the l^∞-norms $|\phi_{,i}|$ and $|\phi_{,ij}|$ for the problems (a) and (b) for a sphere and (c) and (d) for an ellipsoid considered in Section 4.2.1

$\lvert g\rvert$	(a)	(b)	(c)	(d)
$\lvert\phi_{,1}\rvert$	0.50	0.75	0.6	0.501172109
$\lvert\phi_{,2}\rvert$	0.50	1	0.75	0.781250000
$\lvert\phi_{,3}\rvert$	0.50	0.75	0.4	0.355481059
$\lvert\phi_{,11}\rvert$	0	$8/\sqrt{15}$	0	1
$\lvert\phi_{,12}\rvert$	1	$8/\sqrt{15}$	1.5	1.141951010
$\lvert\phi_{,13}\rvert$	1	$5/\sqrt{3}$	0.8	0.536543873
$\lvert\phi_{,22}\rvert$	0	3	0	1.953125000
$\lvert\phi_{,23}\rvert$	1	$8/\sqrt{15}$	1	0.943929861
$\lvert\phi_{,33}\rvert$	0	$8/\sqrt{15}$	0	0.976562500

Table 6
Computed values of the l^∞-norms $|\phi_{,i}|$ and $|\phi_{,ij}|$ for the 2-sphere cluster (with $d = 2$ for (i) and $d = 1.2$ for (ii)) and the 3-sphere cluster with $d = 1.2$ ($l = 1$ and $l = 2$ rows)

$\lvert g\rvert_l$	(i)	(ii)	$l = 1$	$l = 2$
$\lvert\phi_{,1}\rvert_l$	1.01431739	1.05883156	1.14656830	1.17069207
$\lvert\phi_{,2}\rvert_l$	1.01431739	1.05883156	1.16745862	1.05761683
$\lvert\phi_{,3}\rvert_l$	1.04000000	1.08650519	1.11956142	1.11956142
$\lvert\phi_{,11}\rvert_l$	1.98825507	1.96837442	2.06648896	2.16211465
$\lvert\phi_{,12}\rvert_l$	1.50125920	1.51270937	1.70395343	1.72717688
$\lvert\phi_{,13}\rvert_l$	1.50408962	1.52014837	1.53307521	1.54064421
$\lvert\phi_{,22}\rvert_l$	1.98825507	1.96837442	2.62316431	1.91525806
$\lvert\phi_{,23}\rvert_l$	1.50408962	1.52014837	1.53985593	1.50135529
$\lvert\phi_{,33}\rvert_l$	2.07407407	2.72886297	1.93676893	1.93676893

References

[1] H.K. Moffatt, A. Sellier, Migration of an insulating particle under the action of uniform ambient electric and magnetic fields. Part 1. General theory, J. Fluid Mech. 464 (2002) 279–286.

[2] H. Schulz, C. Schwab, W.L. Wendland, The computation of potentials near and on the boundary by an extraction technique for boundary element methods, Comput. Methods Appl. Mech. Engrg. 157 (1998) 225–238.

[3] W.L. Wendland, H. Schulz, C. Schwab, On the computation of derivatives up to the boundary and recovery techniques in BEM, in: H.A. Mang, F.G. Rammerstorfer (Eds.), IUTAM Symposium on Discretization Methods in Structural Mechanics, Kluwer Academic Publishers, 1999, pp. 155–164.

[4] C. Schwab, W.L. Wendland, On the extraction technique in boundary integral equations, Math. Comput. 68 (1999) 91–122.

[5] G. Krishnasamy, F.J. Rizzo, T.J. Rudolphi, Hypersingular boundary integral equations: their occurrence, interpretation, regularization and computation, in: P.K. Banerjee, S. Kobayashi (Eds.), Developments in Boundary Element Methods, Advanced Dynamic Analysis, vol. 7, Elsevier, 1992 (Chapter 7).

[6] J. Hildebrand, G. Kuhn, Numerical computation of hypersingular integrals and application to the boundary integral equation for the stress tensor, Engrg. Anal. Bound. Elem. 10 (1992) 209–218.

[7] M. Guiggiani, G. Krishnasamy, T.J. Rudolphi, F.J. Rizzo, A general algorithm for the numerical solution of hypersingular boundary integral equations, ASME J. Appl. Mech. 59 (1992) 604–614.

[8] M. Guiggiani, Hypersingular formulation for boundary stress evaluation, Engrg. Anal. Bound. Elem. 14 (1994) 169–180.

[9] H.B. Chen, P. Lu, M.G. Huang, F.W. Williams, An effective method for finding values on and near boundaries in the elastic BEM, Comput. Struct. 69 (1998) 421–431.

[10] E.Z. Polch, T.A. Cruse, C.J. Huang, Traction BIE solutions for flat cracks, Comput. Methods Appl. Mech. Engrg. 2 (1987) 253–267.

[11] T.A. Cruse, C.J. Huang, On the nonsingular traction-BIE in elasticity, Int. J. Numer. Methods Engrg. 37 (1994) 2041–2072.

[12] R. Dautray, J.-L. Lions, Analyse mathématique et calcul numérique pour les sciences et les techniques, Masson, Paris, 1988.

[13] G.C. Hsiao, W.L. Wendland, A finite element method for some integral equations of the first kind, J. Math. Anal. Appl. 58 (1977) 449–481.

[14] M. Costabel, Boundary integral operators on Lipschitz domains – elementary results, SIAM J. Math. Anal. 19 (1987) 613–626.

[15] J.-C. Nedelec, Acoustic and Electromagnetic Equations, Integral Representations for Harmonic problems, Springer-Verlag, 2001.

[16] R. Duduchava, The Green formula and layer potentials, Integral Equat. Operator Theory 41 (2001) 127–178.

[17] A. Sellier, Hadamard's finite part concept in dimension $n \geqslant 2$, distributional definition, regularization forms and distributional derivatives, Proc. R. Soc. Lond. A 445 (1994) 69–98.

[18] D.E. Beskos, Introduction to Boundary Element Methods, in: D.E. Beskos (Ed.), Computational Methods in Mechanics, Elsevier Science Publishers, 1987.

[19] C.A. Brebbia, J.C.L. Telles, L.C. Wrobel, Boundary Element Techniques, Theory and Applications in Engineering, Springer-Verlag, Berlin, Heidelberg, New York, Tokyo, 1984.

[20] M. Bonnet, Boundary Integral Equation Methods for Solids and Fluids, John Wiley & Sons Ltd, 1999.

[21] M. Rezayat, D.J. Shippy, F.J. Rizzo, On time-harmonic elastic-wave alaysis by the boundary element method for moderate to high frequencies, Comput. Methods Appl. Mech. Engrg. 55 (1996) 349–367.

[22] J.N. Lyness, D. Jespersen, Moderate Degree Symmetric Quadrature Rules for the Triangle, J. Inst. Math. Appl. A 15 (1975) 19–32.

[23] I.S. Gradshteyn, I.M. Ryzhik, Tables of Integrals, Series and Products, Academic Press, 1965.